Factorized Electron-Nuclear Dynamics with an Eective Complex Potential

Sophya Garashchuk, Julian Stetzler, and Vitaly Rassolov

Department of Chemistry & Biochemistry, University of South Carolina, Columbia, South Carolina 29208

E-mail: garashchuk@sc.edu

Abstract

We present a quantum dynamics approach for molecular systems based on wave-function factorization into components describing the light and heavy particles, such as electrons and nuclei. The dynamics of the nuclear subsystem can be viewed as motion of the trajectories dened in the nuclear subspace, evolving according to the average nuclear momentum of the full wavefunction. The probability density ow between the nuclear and electronic subsystems is facilitated by the imaginary potential, derived to ensure a physically meaningful normalization of the electronic wavefunction for each conguration of the nuclei, and conservation of the probability density associated with each trajectory in the Lagrangian frame of reference. The imaginary potential, dened in the nuclear subspace, depends on the momentum variance in the nuclear coordinates averaged over the electronic component of the wavefunction. An eective real potential, driving the dynamics of the nuclear subsystem, is dened to minimize motion of the electronic wavefunction in the nuclear degrees of freedom. Illustration and the analysis of the formalism are given for a two-dimensional model system of vibrationally nonadiabatic dynamics.

1 Introduction

The importance of nuclear quantum eects (NQE) on reactivity and properties of chemical systems gain recognition in chemistry thanks to advanced innovative experiments covering a wide range of systems from proteins to gas-phase UV-absorption. Some recent representative examples include exciton splitting and vibrational energy pooling in a laser-induced isomerization of a double-well quantum system in the condensed phase (CO adsorbed on NaCl(100) forming OC-Na^+ to CO-Na^+[1]), validation of the quantum rate theories based on measured thermal rates of the hydrogen recombination on platinum crystalline surfaces,[2] contribution of tunneling to the kinetic isotope eect of the intermediate hydrogen transfer step in the Cytochrome P450 Decarboxylase OleT,[3] and the tunneling dynamics, observed in the excited state hydrogen transfer reaction of phenol{ammonia clusters.[4] Practical and conceptually insightful atomistic approaches to dynamics of large systems, characterized by the mass- and time-scale separation, e.g. electron/nuclear dynamics, are typically based on the trajectory description of nuclear motion and the wavefunction description of the electronic motion. The development of inherently consistent yet computationally feasible methods incorporating the NQEs in large systems remains an outstanding challenge and an active research area of theoretical chemistry.

Arguably, the most accomplished method of exact quantum dynamics ([5]) is the multiconguration time-dependent Hartree method (MCTDH).[6{8] Unlike the conventional methods based on direct-product basis representations of wavefunctions, generally limited to systems of 10-12 degrees of freedom (DOFs),[9] the MCTDH is based on the contraction of a general basis to single (or a few) particle functions, which greatly reduces the basis size and numerical cost. The eciency/accuracy balance is further improved within the multilayer version[10] through a simplied description of the spectator modes in a chemical process. The MCTDH has proved especially successful in applications to bound high-dimensional molecular systems, e. g. 15-dimensional simulation of the infrared spectrum of water dimer[11] and tunneling splitting in malonaldehyde.[12,13] A related variational multiconguration Gaussian

approach[14] { its implementation extends to nonadiabatic dynamics with on-the-y evaluation of the electronic structure[15] { employs time-dependent basis functions providing a closer connection between the evolving in time wavefunction and the means to represent it.

When one is willing to trade o exact quantum treatment of the nuclei for an ability to study larger molecular systems, the trajectory representation of the nuclear motion is a long-established framework, which goes all the way to a highly useful classical motion of the nuclei treated as point-particles. A multitude of trajectory-based or trajectory-inspired methods, incorporating the NQEs approximately, often through the trajectory interaction or dynamics in extended spaces, have been developed, such as semiclassical initial value representation,[16,17] ring-polymer molecular dynamics,[18{20] approximate quantum trajectory methods,[21] and approximate path-integral methods.[22] There are trajectory-based yet (in principle) exact methods such as guided Gaussian methods,[23{25] and accurate implementations of the quantum trajectory dynamics.[26{28]

The idea of the time-dependent wavefunction representation is realized not only for the nuclei, but for the electrons as well, in the exact factorization methods, which are actively developed by a number of research groups.[29{31] In these methods the total molecular wavefunction is a product of the time-dependent electronic wavefunction which parametrically depends on nuclear coordinates and a nuclear wavefunction. This method is somewhat similar to the Born-Oppenheimer (BO) approach, but with the nuclear dynamics occurring on a now time-dependent (instead of static) potential energy surface (PES) and with a time-dependent vector potential.[32{34] The main appeal of this approach, is that the nuclear dynamics occur on a single TDPES and time-dependent potential vector, and the exact molecular wavefunction can be given as a single product unlike the Born-Huang approximation where the exact non-adiabatic dynamics and molecular wavefunction requires summations across all electronic states.[35,36] However, while the TDPES provides the exact force acting on the nuclei, obtaining the TDPES is still as dicult and computationally expensive as solving the full TDSE for the electron-nuclear system and, thus, for larger systems approximations must

be made.[33,37]

Here we present a dynamics approach combining certain features of the exact factorization and the quantum trajectory dynamics. Motivated by the mass- and time-scale separation characteristic of electron-nuclear dynamics, we introduce a product form for the full wavefunction with the nuclear component, describing the overall nuclear motion, possibly, in the trajectory framework, and the electronic component, maintaining compatibility with the modern electronic structure methods (ab initio or Density Functional Theory methods using real atom-centered basis sets). An eective real potential driving the dynamics of the nuclear subsystem is dened to minimize the changes of the electronic wavefunction relative to the moving nuclei. The probability density ow between the two subsystems yielding physically meaningful normalization of the wavefunction components, is described by a rigorously derived imaginary potential. The formalism is presented in Section 2. The relative complexity of the equations is due to the non-linear coupling of the nuclear and the electronic components, further complicated by the moving nuclear frame of reference. (The reader is urged to pay attention to the $@_t$ (static Eulerian) vs. $\frac{d}{dt}$ (moving Lagrangian) time derivatives in the dynamic equations.) The results and analysis of Section 3 are based on the time-evolution of a model vibrationally-nonadiabatic system, introduced by Kohen, Stillinger and Tully (KST).[38] It is solved by a Gaussian wavefunction: the dierential equations dening the wavefunction parameters are analytic, yet it cannot be factored into purely electronic and purely nuclear time-dependent components. Thus, it is one of the simplest non-trivial models to test the proposed factorization formalism. Section 4 presents the summary and outlook.

2 Theory

For clarity, the derivation below is given for a two-dimensional system of light (coordinate x) and heavy (coordinate y) particles of masses m and M, respectively, which will be referred to as the 'electron' and 'nuclei'. Obviously, the same framework is applicable to systems

comprised of light and heavy nuclei, such as those characterized by the proton (light particle) transfer within the molecular environment (heavy particles). We adhere to the following notations: the partial time-derivative in the stationary, or Eulerian, frame of reference is labeled as $@_t$. The time-derivative in the frame of reference moving in the nuclear subspace, or the Lagrangian frame, is denoted as d=dt. Variables y_t and p_t are reserved to denote the position and momentum of a trajectory in the nuclear subspace y at time t. The spatial derivatives are labeled as $r_x = @=@x$ and $r_y = @=@y$. Integrals of the two-dimensional functions over the x-coordinate are denoted as $h::: i_x$. The arguments of functions are suppressed when unambiguous, and atomic units (~ = 1) are used throughout. The key notations are summarized in Table 1 for convenience.

Table 1: The key denitions pertaining to the factorized wavefunction evolving in time under the Hamiltonian $\hat{H} = \hat{K}_x + \hat{K}_y + V(x; y)$.

The nuclear wavefunction, (y; t)		
$= j\ j^2$	$p = r_y \arg(\ )$	$r = r_y j\ j=j\ j$
The electronic wavefunction, (x; y; t)		
$N(y) = hji_x r = r_y jj=jj$	$r = hjrj^2_x=N$	$p = {}^2 r_y \arg()$
$p = hjpji_x=N$	$p^2 = hjp^2\ ji_x=N = p^2$	
$\overline{p^2}^{1=2}$	$\hat{D}_1 = r_y \frac{r_y}{M}$	$\hat{D}_2 = \frac{r_y^2}{2M}$
$\hat{K}_x = \frac{r_x^2}{2m}$	$\hat{H}_{el} = \hat{K}_x + V(x; y)$	$E = \frac{1}{N}(hj\hat{H}_{el} i_x + <hjD_2 i_x)$
Full wavefunction, (x; y; t) = (x; y; t) (y; t)		
$P_x = r_x \arg(\ )$	$P_y = r_y \arg(\ )$	$\hat{K}_y = \frac{r_y^2}{2M}$
The nuclear subspace trajectory, $(y_t; p_t)$		
$p_t = p + \overline{p}$	$dy_t=dt = p_t=M$	$w_t = (y_t)y_t$

2.1 The time-dependent Schrödinger equation for a factorized wavefunction

A full-dimensional wavefunction (x; y; t) can be represented in a product form without loss of generality as

$$(x; y; t) = \underbrace{(x; y; t)}_{\text{electronic}} \underbrace{(y_t;)}_{\text{nuclear}} \tag{1}$$

where the function (y; t) will capture the overall nuclear motion and connect to its trajectory description, such as that of the Madelung-de Broglie-Bohm formulation.[26,39] The electronic component at this point is exact, i.e. = = , and depends on both x and y coordinates. We dene p_t, specifying a moving frame of reference in the y-subspace,

$$\frac{d}{dt} = @_t + \frac{p_t}{M} r_y ; \tag{2}$$

such that, rst of all, the continuity equation on the nuclear probability density, , is fullled along the trajectory y_t, evolving in time according to, so far, an unspecied momentum p_t,

$$(y_t) := j \quad (y_t; t) j^2; \qquad \frac{d(y_t)}{dt} = \frac{r_{y_t} p_t}{M} (y_t); \tag{3}$$

$$\frac{dy_t}{dt} = \frac{p_t}{M} : \tag{4}$$

The second requirement on p_t is that the normalization of the electronic component (x; y; t) along the trajectory y_t, i.e. evaluated at $y = y_t$, is constant in time,

$$N(y) := h j i_x; \qquad \frac{dN(y_t)}{dt} = 0: \tag{5}$$

The usual time-dependent Schrödinger equation (TDSE) in the Cartesian coordinates,

$$\hat{K}_x + \hat{K}_y + V(x; y) = \{@_t \; ; \; \hat{K}_x = \frac{r_x^2}{2m}; \; \hat{K}_y = \frac{r_y^2}{2M}; \tag{6}$$

for the wavefunction of Eq. (1) yields:

$$\hat{K}_x + \hat{K}_y + \hat{K}_y \quad \frac{1}{M} r_y \quad r_y + V(x; y) = \{(@_t + @_t): \tag{7}$$

We seek to dene the portion of Eq. (7) { multiplied by a common electronic wavefunction { as the nuclear TDSE, while the remaining portion denes the electronic TDSE (solved by

) with the imposed constraints on the electronic wavefunction described further. The constraints can be divided into those related to the (i) normalization of the factored functions, and (ii) their phase. The former, given by Eq. (5), is intuitive and common to the factorization schemes investigated in this and other works.[29,30,34] Here, however, we also explore factorization schemes leading to dierent partitioning of the wavefunction phase associated with the nuclear motion.

The wavefunction factorization is achieved by adding and subtracting in the TDSE (7) a complex time-dependent potential, V_d, dened in the nuclear subspace,

$$V_d := V_r(y;t) + \{V_i(y;t); \tag{8}$$

where V_r and V_i are its real and imaginary parts. Then, Eq. (7) can be rearranged as:

$$\underbrace{\left(\hat{K}_y + V_d\right) \{@_t}_{=0;\ \text{nuclear TDSE}} + \underbrace{\hat{K}_x + \hat{K}_y \quad \frac{1}{M}\frac{r_y}{r_y} + V \quad V_d \quad \{@_t}_{=0;\ \text{electronic TDSE}} = 0: \tag{9}$$

Denoting the electronic Hamiltonian $\hat{H}_{el}$,

$$\hat{H}_{el} = \hat{K}_x + V(x;y); \tag{10}$$

and the rst and second derivative operator terms, respectively, as

$$\hat{D}_1 := \frac{r_y}{} \frac{r_y}{M} \tag{11a}$$

$$\hat{D}_2 := \frac{r_y^2}{2M}; \tag{11b}$$

Eq. (9) yields the nuclear and electronic TDSEs, respectively,

$$\hat{K}_y + V_d = \{@_t ; \tag{12}$$

$$\hat{H}_{el} + (\hat{D}_2 + \hat{D}_1) \qquad V_d = \{@_t: \tag{13}$$

The operators $\hat{D}_2$ and $\hat{K}_y$ are formally the same, but, as common in the literature, the former notation will be used henceforth for the nuclear kinetic energy of the electronic wavefunction.

At this point let us note that, unlike the exact factorization method,[33,34] V_d is the only introduced 'object', which is a complex scalar function, not a dierential operator or vector potential. Restricting V_d to be a function is a limitation of the nuclear/electronic equation 'decoupling' scheme above, which is, nevertheless, formally exact. Furthermore, as shown in the remainder of this section, the normalization constraints are achieved by imposing conditions on V_i, which dene it uniquely, while V_r controls the electron/nuclear phase partitioning. It is not unique, but a well-dened procedure of dening V_r is established. Also note, that the derivative operators, $\hat{D}_1$ and $\hat{D}_2$, in Eq. (13) are, in general, non-Hermitian in the electronic subspace. Thus, the electronic norm, $N(y)$, is not guaranteed to stay constant in time. However, the electronic norm conservation and the continuity equation for the nuclear density (Eqs (3) and (5)) can be satised if the potential V_d is a complex function as shown below.

2.2 Denition of the imaginary part of the dynamics potential

The continuity of the nuclear probability density. Using $(y;t)$ in the polar form,

$$(y;t) = j \quad (y;t)j \exp(\{\arg(\quad (y;t))); \tag{14}$$

dening the corresponding probability density, $(y;t)$, and the phase gradient, or the quantum trajectory (QT) momentum, $p \quad (y;t)$[26] as,

$$:= j \quad (y;t)j^2; \qquad p \quad := r_y(\arg \quad (y;t)); \tag{15}$$

the continuity equation for , following from Eq. (12), is:

$$\partial_t + \frac{p}{M}\nabla + \frac{\nabla_y p}{M} \quad 2V_i = 0: \tag{16}$$

Upon switching to the Lagrangian frame of Eq. (2), specied by an unknown so far p_t, Eq. (16) becomes,

$$\underbrace{\partial_t + \frac{p_t}{M}\nabla}_{d=dt} + \underbrace{\frac{\nabla_y p_t}{M}}_{=0;\ \text{continuity eq}} \quad \underbrace{\frac{\tilde{p}}{M}\nabla \quad \frac{\tilde{p}}{M} \quad 2V_i}_{=0;\ \text{condition on } p_t \text{ and } V_i} = 0: \tag{17}$$

Here $\tilde{p}$ denotes the dierence between p_t and p , the latter associated with the phase of $(y; t)$,

$$\tilde{p} := p_t \quad p : \tag{18}$$

As follows from Eq. (17), the continuity equation on in the Lagrangian frame is fullled for the following V_i,

$$V_i := \frac{\tilde{p}\nabla}{2M} \quad \frac{\nabla\tilde{p}}{2M}; \tag{19}$$

where the function $\tilde{p}$, related to p_t, is so far undened. Similar to the QT dynamics[40] the continuity equation implies that the trajectory weights, dened as the probability density within the volume element, y_t, associated with the trajectory $(y_t; p_t)$, are conserved,

$$w_t := (y_t; t)y_t; \qquad \frac{dw_t}{dt} = 0: \tag{20}$$

The electronic wavefunction norm. Now let us consider the probability density ow of the electronic part. Given the time-evolution Eq. (13), jj^2 changes as

$$\partial_t jj^2 = \{H_{el} \quad \{(D_2 + D_1) + \{V_d jj^2 + \{(H_e^{\dagger}) + \{((D_2 + D_1)) \quad \{V jj^2: \tag{21}$$

Integration of Eq. (21) over the electronic DOFs species the time-dependence of the electronic norm, $N(y)$ of Eq. (5), in the Eulerian frame,

$$\partial_t N(y) = \{(\langle\chi|(\hat{D}_1 + \hat{D}_2)|\chi\rangle_x \qquad \langle\chi|(\hat{D}_2 + \hat{D}_1)|\chi\rangle_x \qquad 2V_i N(y): \tag{22}$$

In the Lagrangian frame, at $y = y_t$, Eq. (22) becomes,

$$\frac{d}{dt}N(y_t) = 2\Re\left[\langle\chi|(\hat{D}_2 + \hat{D}_1)|\chi\rangle_x\right]_{y=y_t} \qquad 2V_i N(y_t) + \frac{p_t}{M}\partial_y N(y_t): \tag{23}$$

Setting Eq. (23) to zero and using the polar form of , one obtains:

$$V_i = \frac{\Re\left[\int \chi^* \partial_y(|\chi|^2)dx \qquad \partial_y\left(\int |\chi|^2 \partial_y(\arg\chi)dx\right) \qquad \partial_y \int |\chi|^2 \partial_y(\arg\chi)dx\right]_{y=y_t} 2M N(y_t)}{}: \tag{24}$$

Let us denote the y-component of the momentum associated with the electronic wavefunction, p, and the relevant averages normalized with respect to x, as

$$p := \partial_y(\arg\chi); \qquad \overline{p} := \frac{\int p|\chi|^2 dx}{N(y)}; \quad \overline{p^2} := \frac{\int p^2|\chi|^2 dx}{N(y)} \tag{25}$$

The gradient of $\overline{p}$ is

$$\nabla(\overline{p}) = \frac{\partial_y\left(\int p|\chi|^2 dx\right)}{\underbrace{N(y)}_{\partial N(y)=N(y)}} - \frac{\partial_y\left(\int |\chi|^2 dx\right)}{N(y)}\underbrace{\frac{\int p|\chi|^2 dx}{N(y)}}_{\overline{p}}: \tag{26}$$

Expressing $\partial_y\left(\int p|\chi|^2 dx\right)$ from Eq. (26), Eq. (24) yields another expression for V_i:

$$V_i = \frac{(\overline{p^2} - \overline{p})\,\partial_y N(y_t)}{2M\,N(y_t)} - \frac{\partial p}{2M} - \frac{p\,\partial_i}{2M}: \tag{27}$$

The two denitions of V_i { Eqs (19) and (27) derived from the requirements on the probability densities of Eqs (3) and (5), respectively, { are equivalent if

$$p_e = \overline{p}: \tag{28}$$

This means that (from Eq. (18)) the trajectory evolves according to the nuclear momentum p_t of the full wavefunction , averaged and normalized over the electronic DOFs,

$$p_t = p + \overline{p}\,\hbar \frac{j r_y(\arg)j \quad i_x}{\hbar \; j \quad i_x}: \tag{29}$$

Denition of the initial wavefunction. The purpose of the desired factorization is to incorporate the nuclear momentum of the full (two-dimensional) wavefunction into the nuclear component (one-dimensional) , as much as possible. Thus, ideally, the nuclear wavefunction is chosen such that $\overline{p}$ (which is the normalized x-averaged nuclear momentum of the electronic wavefunction) is equal to zero. This can be accomplished by requiring

$$\frac{r_y \quad (y;0)}{(y;0)} = z(y;0); \tag{30}$$

where z is the x-averaged log-derivative of ,

$$z(y;0) = \frac{\int (x;y;0) r_y \quad (x;y;0)dx\, j}{\int (x;y;0)j^2 dx}: \tag{31}$$

According to Eqs (30) and (31), for a single nuclear DOF (y;0) can be dened as

$$(y;0) = N \quad \exp \int_1^y z(y^0;0)dy^0 \quad ; \tag{32}$$

where N is the appropriate normalization constant ($\int$ j (y; 0)j^{2}dy = 1). Then, $\overline{p}$ (Eq. (25)) and $r_y N(y)$ of the corresponding initial electronic wavefunction (x; y; 0),

$$(x; y; 0) = \frac{(x; y; 0)}{(y; 0)}; \tag{33}$$

are equal to zero by construction. The latter condition means that the resulting electronic normalization is uniform, i. e. N(y; 0) = const.

Summary. So far, based on Eqs (19) and (27), we have shown that the desired probability conservation properties, i.e. the constant-in-time electronic norms, f$N(y_t)$g, and the nuclear trajectory weights, fw_tg, are fullled in the Lagrangian frame, dened by p_t of Eq. (29), i.e. by the nuclear momentum of the full wavefunction averaged and normalized with respect to the electronic DOFs, in the presence of a specic imaginary part of V_d:

$$V = \frac{r_y \overline{p}}{2M} \quad \frac{\overline{p}\, r_y j \quad j^{i}}{M \; j \quad j}: \tag{34}$$

As shown in Appendix A, the counterparts to fw_tg dened for the full wavefunction (x; y_t; t) are constant in time as well. Note, that V_i above is consistent with simply setting the imaginary part of the x-averaged electronic TDSE (13) to zero, yielding V_i = =(hj(D_2^+ $\hat{D}_1$)i_x). Furthermore, for a uniformly normalized electronic wavefunction, which means $r_y N(y_t)$ = 0, V_i of Eq. (34) does not depend on the frame of reference, because switching to any moving frame would add a term proportional to r_y N to Eq. (23), from which the V_i denition follows. Lastly, the nuclear subspace factorization of Eqs (31{32) is applicable to any wavefunction. In other words, the procedure does not depend on the factorizability of the full wavefunction and can be performed at any time generating the optimal (in a sense of having $\overline{p}$ = 0) (y; t) in the one-dimensional nuclear subspace. The dynamics and associated quantities yielding $\overline{p}$ = 0 at all times will be referred to as 'optimal' henceforth.

2.3 Denition of the real part of the dynamics potential

In Section 2.2 we have derived the imaginary part $V_i(y)$ (Eq. (34)) of the potential $V_d(y)$, the latter introduced to 'uncouple' the nuclear and electronic TDSEs for a factorized wave-function. We have also demonstrated that the imposed probability conservation properties do not depend on its real part, $V_r(y)$, which denes the time-evolution of the nuclear wave-function, in particular, its phase. This independence is related to a non-unique assignment of the y-dependent phase to the two wavefunction components, i.e. adding a phase to and subtracting the same from does not change the full wavefunction . In this section we consider some choices of V_r, which in some sense minimize motion of in the nuclear coordinate, y, by generating the dynamics characterized by small $\overline{p}$ and its gradient, and, consequently, by small V_i.

Reducing the time-dependence of the electronic energy. First, let us dene V_r by minimizing the change of the electronic wavefunction energy, given by the TDSE (13). Its x-averaged value can be set to zero in either the Eulerian or Lagrangian frames of reference, i.e $\hbar\partial_t \arg i_x = 0$ or $\hbar\frac{d}{dt}\arg i_x = 0$, respectively. (To switch to the Lagrangian frame of reference an operator $\{p_t r_y/M$ is added to both sides of Eq. (13).) Referring to the imaginary and real components of r_y = in the derivative coupling operator $\hat{D}_1$ as p (Eq. (15)) and r { both functions of y and t,

$$r \quad := \frac{r_y j \quad j}{j \quad j}; \tag{35}$$

and to the sum of the second derivative term and electronic energy as E, one obtains:

$$V_r^{eul} = E + \frac{p \quad \overline{p}}{M}; V \tag{36a}$$

$$_r^{lagr} = E \quad \frac{(p)^2}{M}; \tag{36b}$$

$$E := \frac{hjH_{el}^{\wedge}ji_x}{N(y)} + \frac{<(hjD_2^{\wedge}ji_x)}{N(y)}: \tag{36c}$$

Both forms of V_r above can be interpreted as counterparts to V_i derived in Section 2.1, which eectively sets the imaginary part of x-averaged Eq. (13) to zero. However, now there is an explicit dependence on the frame of reference: V_r^{eul} does not take into account the nuclear motion, and in V_r^{lagr}, dened by p_t of Eq. (29), the terms associated with $D_1^{\wedge}$ formally cancel. While the whole point of considering moving frames of reference is to reduce coupling between the electronic sub-packets, $f(x; y_t; t)g$, associated with each y_t (so the coupling is amenable to approximations), we expect these sub-packets to, at least, exchange energy due to the rst derivative coupling along the nuclear DOF, explicitly expressed via p term in Eq. (36a) and absent in Eq. (36b). Thus, both forms of V_r given by Eqs (36a) and (36b) might be sub-optimal in a sense of generating complicated nuclear dynamics and large imaginary potentials. Therefore, we also consider an intermediate denition of V_r, associated with the 'electronic' moving frame, which incorporates the average motion of the electronic wavefunction in the nuclear DOF, by replacing p_t in Eq. (2) with $\overline{p}$:

$$V_r^{el} = E + \frac{\overline{p}\overline{p}}{M} \quad \frac{(\overline{p})^2}{M}: \tag{37}$$

So far, based on the energy minimization, we have argued for three choices of V_r specied by Eqs (36a, 36b) and (37).

Reducing the nuclear momentum of the electronic wavefunction. Next, let us construct V_r, which 'minimizes' $\overline{p}$ and its gradient during the dynamics, using the time-dependence of $\overline{p}$. Since $\overline{p}$ depends on the nuclear momentum of the full wavefunction (Eq. (7)), we begin with its equation of motion. Denoting

$$P_x := r_x(\arg \quad); \quad P_y := r_y(\arg \quad); \tag{38}$$

for given in terms of its modulus and phase yields TDSE (6) (see e.g.[26]),

$$@_t P_y = \quad r_y (V + U) \quad \frac{P_x}{m} r_x P_y \quad \frac{P_y}{M} r_y P_y ; \tag{39}$$

where U is the quantum potential for the full wavefunction,

$$U := \frac{r_x^2 j \quad j}{2m j \quad j} \quad \frac{r_y^2 j \quad j}{2M j \quad j} : \tag{40}$$

As shown in Appendix B, combining Eq. (39) with its counterpart for $r_y(\arg \quad)$ setting the resulting time-derivatives of $\overline{p}$ to zero, one obtains the following expressions for $r_y V_r$, 'minimizing' the electronic motion in the Eulerian and Lagrangian frames of reference:

$$(r_y V_r)^{eul} = G + \frac{r_y (\overline{p})^2}{2M} + \frac{r_y (p \quad p)}{2M} ; \tag{41a}$$

$$(r_y V_r)^{lagr} = G + \frac{\overline{p}}{M} r_y p \quad ; \tag{41b}$$

where G stands for

$$G := \frac{h j r_y V j i_x}{N(y)} + \frac{(2r \quad + r_y)(\overline{r^2} + \quad ^2) M}{} : \tag{42}$$

In Eq. (42) and throughout the 'non-classical' momentum components, r given by Eq. (35) and r,

$$r := \frac{r_y j j}{j j} ; \qquad \overline{r^2} = \frac{h j r j i_x^2}{N(y)} ; \tag{43}$$

associated with the nuclear and electronic wavefunctions are used. The function ^{2} denotes the nuclear momentum dispersion (variance), which is the same whether computed for the full wavefunction or for the electronic component :

$$:= \overline{p} \quad _2 \quad (p)^2 \quad ^{1=2} : \tag{44}$$

A few notable features of Eqs (41a) and (41b) are: (i) they dene forces which, in general, cannot be integrated to yield V_r which is a scalar function; (ii) unlike for V_r^{lagr} of Eq. (36b), $(r_y V_r)^{lagr}$ explicitly contains the electron-nuclear momentum coupling, and (iii) there is no contribution from the kinetic energy in the electronic coordinate. Therefore, in the numerical tests presented in Section 3.3, we consider denitions for V_r of Eqs (36a, 36b) and (37) with and without the kinetic energy terms associated with the action of $\hat{K}_x$ and $\hat{D}_2$ on .

The stationary condition on the x-averaged electronic wavefunction. Finally, we show that it is possible to keep the average nuclear momentum of the electronic wavefunction, $\overline{p}$, equal to zero, and, in case of a single nuclear DOF, a unique (up to a constant) purely real eective potential of Eq. (8), $V_i = 0$ and $V_d = V_r$, can be constructed. In this limit the wavefunction factorization in our approach becomes unique, which is similar to the exact factorization method, where (in the same limit of a single nuclear DOF) the vector potential is equal to zero and the dynamics is driven by a real scalar potential.[33,34,41]

First, for electronic functions = jj exp({ arg()), normalized to 1 at all times, the x-averaged nuclear momentum, $\overline{p}$ (Eq. (25)), can be computed via a simple linear operator,

$$\{hr_y i_x = \{hjjr_y jji_x + hjjr_y(\arg)jji_x = \frac{\{}{2} r_y(N(y)) + pN(y) = p: \overline{} \qquad (45)$$

The last equality in Eq. (45) holds if N(y) 1. The time-dependence of p $\overline{\text{can}}$ now be computed from the time-dependence of given in Eq. (13):

$$\begin{aligned} \{@_t\overline{p} &= h(\ \{)(\hat{H}_{el} + (\hat{D}_1 + \hat{D}_2 \quad V_r))jr_y i_x + hjr_y(\ \{)(H_{el} + (\hat{D}_1 + \hat{D}_2 \quad \hat{} \quad V_r))ji_x \\ &= \{hj[\hat{H}_{el} \quad V_r; r_y]ji_x + \{hj(D_1 + D_2)r_y \overset{!}{} \quad r_y(\overset{!}{D}_1 \overset{!}{+} D_2)\overset{!}{j}i_x \end{aligned} \qquad (46)$$

where in the last line the direction of action of the derivative operators is explicitly indicated. The derivatives are taken with respect to the (nuclear position) parameter, which is not integrated over in the hi_x notation. Therefore, we carefully keep track of the complex

conjugation of these operators and their commutation with the nuclear gradient. Moreover, the $\hat{D}_1$ term of Eq. (11b) may not be equal to its complex conjugate through the complexity of the nuclear function , hence its complex conjugation is shown explicitly in Eq. (46). The following expressions are nevertheless straightforward to derive:

$$hj(D_2 r_y \quad D_2 r_y)ji^x = \quad 2r_y(hjD_2ji_x\hat{)} \tag{47a}$$

$$hj(D_1 r_y \quad r_y D_1)ji_x = \quad 4r \ hjD_2ji_x\hat{:} \tag{47b}$$

Using these expressions and simplifying the commutator, Eq. (46) yields

$$@_t\overline{p} = \quad hjr_yV ji_x \qquad (4r \ + 2r_y)\, hjD_2\hat{j}i_x + r_yV^r : \tag{48}$$

Setting the above Eq. (48) to zero denes the optimal r_yV_r,

$$r_yV^r = hr_yV i_x + (4r \ + 2r_y)h\hat{D}_2 i_x = hr_yV i_x + \frac{1}{M}(2r \ + r_y)\, hr^2 + pi_x^2: \tag{49}$$

The polar form of has been used in the last equality, and the averages are computed for . Equation (49) is equivalent to Eqs (41a) and (41b) in the limit of $p = 0$, the last two becoming identical in this case.

Summary. (i) The full electron-nuclear wavefunction $(x; y; t)$ can be uniquely represented as a product of the moduli of the nuclear, $(y; t)$, and the electronic, $(x; y; t)$, components, but this factorization is not unique with respect to the full wavefunction phase which depends on the real potential V_r. (ii) Based on the arguments for the energy time-dependence and exchange between the electronic wavefunctions associated with dierent congurations of the nuclei, we have derived several expressions for V_r: V_r^{eul} of Eq. (36a) in the stationary Eulerian frame of reference, V_r^{lagr} of Eq. (36b) in the Lagrangian frame dened by the nuclear momentum of the full wavefunction (averaged and normalized over

with respect to the electronic DOF, x), and V_r^{el} in the moving 'electronic' frame specied by $\overline{p}$, which is the nuclear momentum of the electronic wavefunction averaged over the electronic DOF. (iii) While minimizing the time-dependence of $\overline{p}$ in the Eulerian and in the Lagrangian frames, we have obtained expressions for $r_y V^r$ in which the electronic kinetic energy terms cancel. Therefore, in the numerical study of Section 3, dynamics with V_r^{eul}, V_r^{lagr} and V_r^{el} with and without the kinetic energy terms are considered. While there is no unique denition for V_r, all choices are well-dened for any number of nuclear DOFs. (iv) Finally, we have demonstrated that for one nuclear dimension the electron/nuclear factorization is uniquely dened throughout the dynamics for the 'optimal' V_r, consistent with Eq. (49), and both V_i and $\overline{p}$ are equal to zero at all times. The dynamics for this choice, referred to as V_r^{opt}', is considered in the system study below as well.

3 Results and Discussion

To better understand the formal properties of the dynamics presented in Section 2 we examine the model of Kohen, Stillinger and Tully (KST)[38] of the vibrationally nonadiabatic dynamics, and compare the key dynamics features following from various choices of V_r (Eqs (36a), (36b), (37), (49)), and the analytical denition of V_i (34). The full wavefunction (x; y; t) solving this model is a two-dimensional Gaussian wavepacket evolving in time under a real potential, V (x; y). The nuclear wavefunction (y; t) is a one-dimensional Gaussian evolving in a complex parabolic potential. The electronic wavefunction (x; y; t) is simply dened as a ratio = = , using the Gaussian wavepacket parameters solved for numerically. Generalization of the multidimensional Gaussian wavepacket dynamics[42] to a complex parabolic potential, given in Appendix C, provides the necessary equations of motion for all the parameters. This model allows us to analyze the dynamics with various V_r, decoupling the electron and nuclear TDSEs for an inherently non-adiabatic process bypassing the challenges of general implementation, deferred to future work.

3.1 The model and its key dynamics features

The two-dimensional KST model of the vibrationally-nonadiabatic dynamics[38] can be interpreted as the Hooks atom whose nucleus is conned by a harmonic potential,

$$V = \frac{k(x \quad y)^2}{2} + \frac{Ky^2}{2}: \tag{50}$$

Following prior work we consider the particle masses of $m = 1$ and $M = 10$ a.u. for the 'electronic' coordinates x and 'nuclear' coordinate y, respectively. The initial wavefunction is coupled and complex; the parameter values are listed in Table 2. All values are given in the appropriate atomic units. The full wavefunction is a two-dimensional Gaussian function,

Table 2: The model and initial wavefunction parameters in atomic units. N_{tr} and dy are the number and spacing for the trajectories at time $t = 0$. The parameters are given in appropriate atomic units.

Full wavefunction, $(x; y; 0)$					
k	K	x^c	p_x^c	y^c	p_y^c
5	15	1.0	0.2	1.0	2.0
$<(a_{11})$	$=(a_{11})$	$<(a_{22})$	$=(a_{22})$	$<(a_{12})$	$=(a_{12})$
2.236	0.5	7.142	0.50	-1.0	0.5
The nuclear wavefunction, $(y; 0)$					
Y	P	$<()$	$=()$	N_{tr}	dy
1.0	2.0	6.695	0.724	9	0.45

$$(x; y; t) = e^{\quad a_{11}(x \quad x^c)^2=2 \quad a_{12}(x \quad x^c)(y \quad y^c) \quad a_{22}(y \quad y^c)^2=2+\{p_x^c(x \quad x^c)+\{p_y^c(y \quad y^c)+\{s+g}; \tag{51}$$

specied by the width parameters forming a symmetric matrix A, its elements $fa_{11}; a_{22}; a_{12}g$ being complex functions of time. The overall phase s and normalization constant g are real functions of time. The equations of motion for all parameters follow from expressions in Appendix C for $V_i = 0$, in which case the Gaussian center parameters, $fx^c; y^c; p_x^c; p_y^c g$, describe a classical trajectory. The nuclear function, $(y; t)$, is a one-dimensional Gaussian

with the complex time-dependent width parameter :

$$(y;t) = e^{(y \quad Y)^2=2+\{P(y \quad Y)+\{+} : \tag{52}$$

The equation of motion for and for the real time-dependent parameters, fY; P; ; g, follow from those of Appendix B for the complex potential.

The main dynamics features of this system are shown in Fig. 1. Note that for the chosen initial conditions, the dynamics cannot be reduced to that of uncoupled eective modes. The position of the full wavefunction center as a function of time is displayed in Fig. 1(a). The particle executes nearly harmonic motion in y (the heavy particle DOF), while its motion along x (the light particle DOF) is signicantly perturbed from the harmonic by the coupled potential and initial conditions. An ensemble of N_{tr} = 9 trajectories, initially spaced at 0.45 a_0, tracks the projection of the full-dimensional on the y-subspace (Fig. 1(c)): they are dened by the nuclear component of the full wavefunction averaged over the electronic DOF (dy_t=dt = p_t=M, p_t is given by Eq. (29)). The position of the central trajectory started at the GWP center matches the dynamics of y^c at all times, while the changes in the trajectory spacing over time reect the breathing motion of projected on the y-coordinate. This dynamics conserves the normalization of the electronic wavefunction and the nuclear probabilities, or trajectory weights w_t = j $(y_t)j^2y_t$, along the trajectories in the y-subspace.

The real parts of the wavefunction width parameters $fa_{11}; a_{12}; a_{22}g$ are shown in Fig. 1(b). The initial parameter $<(a_{22})$ was taken to be one-half of the coherent Gaussian value to emphasize the breathing motion of the nuclear wavepacket in the nuclear coordinate y. Thus, $<(a_{22})$ exhibits four-fold variations over time. The cross-term $<(a_{12})$ shows appreciable amplitude variation as well. The parameter $<(a_{11})$ which initially matched the coherent wavepacket width in x exhibits relatively mild variations in time, yet the projections of (x; y; t) onto the instantaneous vibrational states in x illustrate the strongly nonadiabatic

character of this model dynamics due to spatial delocalization of the correlated in x and y Gaussian wavefunction. The time-dependent vibrational state populations, dened as $\%_n = jh\ (x; y^c; t)j_n(x; y^c)i_x j^2$, where $_n$ are the eigenstates of $H_{el} \hat{=} K_x \hat{+} V(x; y^c)$, are shown in Fig. 1(d) for the vibrational quantum numbers n = f0; 1; 2; 3; 4g: the populations of the excited states change from zero to up to 33; 17; 8 and 3 %, respectively.

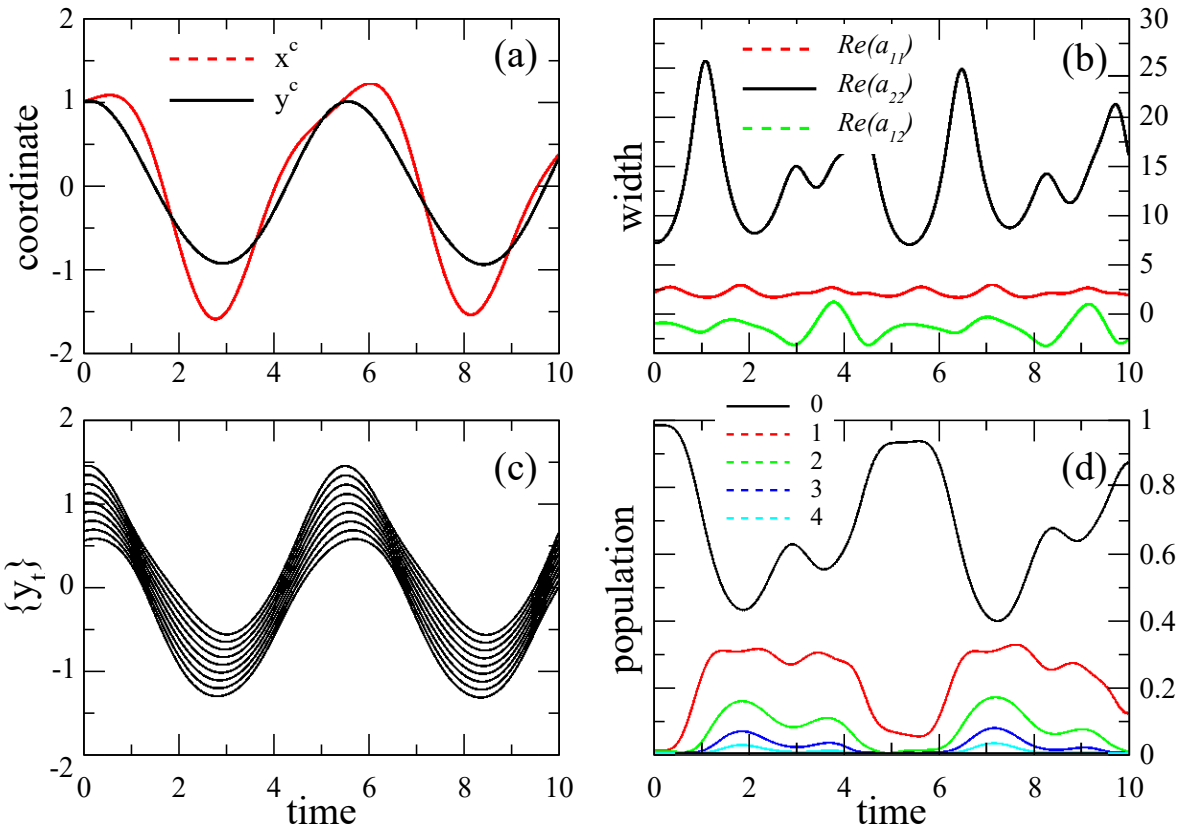

Figure 1: Vibrationally non-adiabatic dynamics of a Gaussian in the KST model. (a) The center posi-tion $(x^c; y^c)$, equivalent to the average position computed over $(x; y; t)$. (b) The real parts of the width matrix elements, $fa_{11}; a_{22}; a_{12}g$. (c) The trajectories, projecting $(x; y; t)$ to the nuclear subspace y, generated according to the x-averaged momentum of the full wavefunction, Eq. (29). (d) Populations of the instantaneous electronic energy eigenstates; the vibrational quantum number is indicated in the legend.

3.2 Dynamics with real mean-eld potential

First let us examine a conventional mean-eld dynamics under the purely real V_d, dened by (i) the total electronic energy or by just (ii) the average classical potential,

$$V_{N(y)}^{(i)} = \frac{hjH_{el}^{\wedge}ji_x{}^d}{hjV}; \tag{53a}$$

$$V_d^{(ii)} = \frac{ji_x}{N(y)}: \tag{53b}$$

Note, that in both cases V_i is zero and $N(y)$ is time-dependent. The average position (Fig. 2(a)) of the nuclear wavepacket and its width (Fig. 2(b,d)) are shown alongside their counterparts obtained from the full wavefunction, . As seen from the gure, the trends for these parameters look somewhat similar, but the deviations are apparent. While the width of is not expected to match the y-component of the full two-dimensional wavefunction width because of the cross-term in the latter, the mismatch between the center of the nuclear wavepacket $Y(t)$ with respect to y^c of the full wavepacket is signicant. As a result of their relative shift, the electronic wavefunction dened as the ratio, = = , becomes very large with time. Since $V_i = 0$, i.e. the electronic norm conservation is not fullled, the trajectory weights $fw_t g$ computed along the trajectories, which are the same as in Fig. 1(c), depend on time. As shown in Fig. 2(c) the values of w_t (plotted on the logarithmic scale) drop to 10^{12} and 10^{8} for the potentials of Eqs (53a) and (53b), respectively. The total nuclear probability is conserved along the trajectories by construction. Thus, the normalization, $N(y_t)$, of each electronic sub-packet centered at y_t is inversely proportional to w_t and compensates the behavior of the latter by acquiring very large values. We also note that the dynamics with $V_d^{(ii)}$ dened by the average potential (Eq. (53b)) yields w_t and $N(y_t)$ that are less singular compared to $V_d^{(i)}$ based on the total electronic energy (Eq. (53a)); this eect may be model-specic.

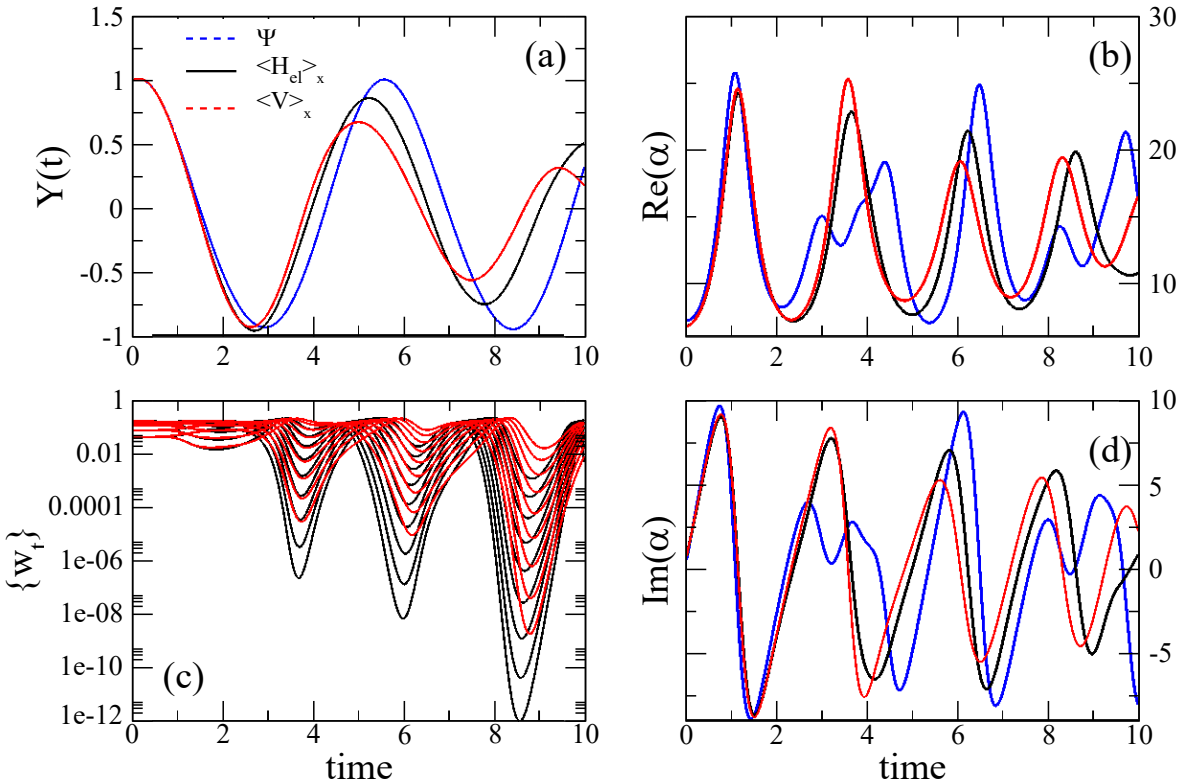

Figure 2: Dynamics with the real mean-eld potentials. (a) The Gaussian center Y (t), and (b) the real and (d) imaginary width parameter of the nuclear wavefunction (y; t). (c) The trajectory weights $\{w_t\}$, which are inversely proportional to the electronic normalization $\{N(y_t)\}$, are shown on the logarithmic vertical scale. In all panels the properties obtained from (y; t) evolving under the average electronic energy (Eq. (53a) and the average potential energy (Eq. (53b) are shown as black lines (label '$\langle H_{el} \rangle$') and red dashes (label '$\langle V \rangle_x$'), respectively. In panels (a,b,d) blue dot-dashes (label ' ') show y^c, $\langle(a_{22})$ and $\overset{x}{=}(a_{22})$, respectively, which are the parameters of (x; y; t) evolving under the full V (x; y).

3.3 Dynamics with the norm-conserving complex potential

Now let us turn to dynamics with the norm-conserving V_i, starting with the full denition of V_r in the Eulerian frame as given by Eq. (36a). As argued in Section 2.3(b), we also consider V_r without the electronic kinetic energy ($\hat{K}_x$) contribution, and without both contributions from the kinetic energy operators ($\hat{K}_x$ and $\hat{D}_2$) of the electronic wavefunction. The results obtained with these three versions of V_r are shown in Figs 3, 4(a,b) and 5(a,b), and labeled as $V^{(0)}$, $V^{(1)}$ and $V^{(2)}$, respectively. Their performance is evaluated based on the time-dependence of the center of the nuclear wavefunction Y (t) (Fig. 3(a)), the momentum P (t) at the center of (Fig. 4(a)), the real and imaginary width parameters of (Figs 3(b) and 4(b), respectively), and the average value and the dispersion of the y-momentum of the electronic wavefunction (Fig. 5(a) and (b), respectively). Wherever appropriate, the full-dimensional counterparts to the quantities obtained from are shown with black solid lines, labeled ' ' in legends. All -specic quantities are shown alongside the optimal analytic nuclear wavefunction ^{opt}, obtained from the full wavefunction by performing a procedure described in Section 2B(c). Let us point out here that $^{opt}(y;t)$, constructed as the normalized x-averaged value of the full wavefunction (x; y; t) for any t, is the same as (y; t) (up to a coordinate-independent phase) computed with the optimal real V_r of Eq. (49) with the integration constant set to zero. The resulting functions are marked with red circles in all panels.

First of all, we note that for the rigorously derived V_i of Eq. (34), the trajectory weights and electronic wavefunction normalization remain constant in time, and that Y (t) = hy(t)i evolving according to the full wavefunction momentum, $p_t = p + \overline{p}$, is the same for all versions of V_r. As seen in Fig. 3(b), the real width parameters <() associated with dierent V_r are nearly the same and close to the optimal value. (Therefore, Y (t) and <() are not plotted for other types of V_r.) In all cases <() deviates from the two-dimensional parameter $<(a_{22})$ (black line) as expected, since is a mapping of the correlated two-dimensional Gaussian to one dimension. In contrast, the phase-related features, i.e. the momentum P (t)

and imaginary width parameter, =(), show signicant dependence on V_r. Features of the dynamics with $V^{(2)}$ (no kinetic energy associated with) are the closest to those from the optimal ^{opt}. Both P(t) and <() obtained from ^{opt} show excellent { perfect in case of P(t) { correlation with their counterparts from the conventional two-dimensional dynamics. The same can be said of the x-averaged motion of the electronic wavepacket (x; y; t) along the nuclear coordinate. The average p and its dispersion (^{2} according to Eq. (44)) are shown in Fig. 5(a,b). Both quantities computed from the dynamics under $V^{(0)}$ and $V^{(1)}$ grow in time despite the bound character of the two-dimensional Gaussian wavepacket motion.

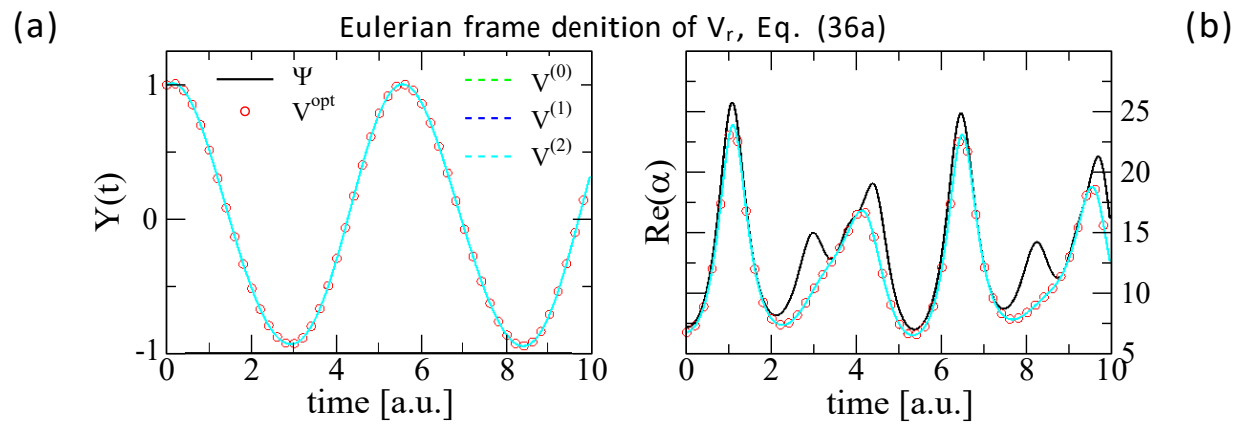

Figure 3: Dynamics with the complex norm-conserving potential dened in the Eulerian frame (Eq. (36a)). (a) The average positions and (b) the real width parameters of the nuclear wavepacket (y; t) are shown as functions of time. The results from the dynamics with all terms in V_r included ($V^{(0)}$), the electronic kinetic energy dropped ($V^{(1)}$) and all kinetic energy dropped ($V^{(2)}$) are shown as green dash, blue wide dash and cyan dot-dash, respectively. The same quantities computed for the optimal (y; t) according to Eq. (49) are indicated with red circles (V^{opt} in legend), while their counterparts y^c and <(a_{22}) of the full wavefunction (x; y; t) are shown with black solid lines (in legend) in (a) and (b), respectively. The same legend applies to both panels. All quantities are given in the appropriate atomic units.

Next, let us examine the dynamics with V_r dened in the Lagrangian frame of reference by Eq. (36b) ($V^{(0)}$) with the same modications (neglecting with $\hat{K}_x$ denes $V^{(1)}$, and with both $\hat{K}_x$ and $\hat{D}_2$ denes $V^{(2)}$) that were tested in the Eulerian frame. The results are displayed in Figs 4(c,d) and 5(c,d). The trends for the various V_r options are largely the same as in the case of the Eulerian frame discussed above. Comparing the dynamics with $V^{(0)}$ and $V^{(1)}$ dened in the Eulerian and Lagrangian frames, we observe that P(t) and average p are somewhat closer to the optimal values in the latter case, while =() and dispersion

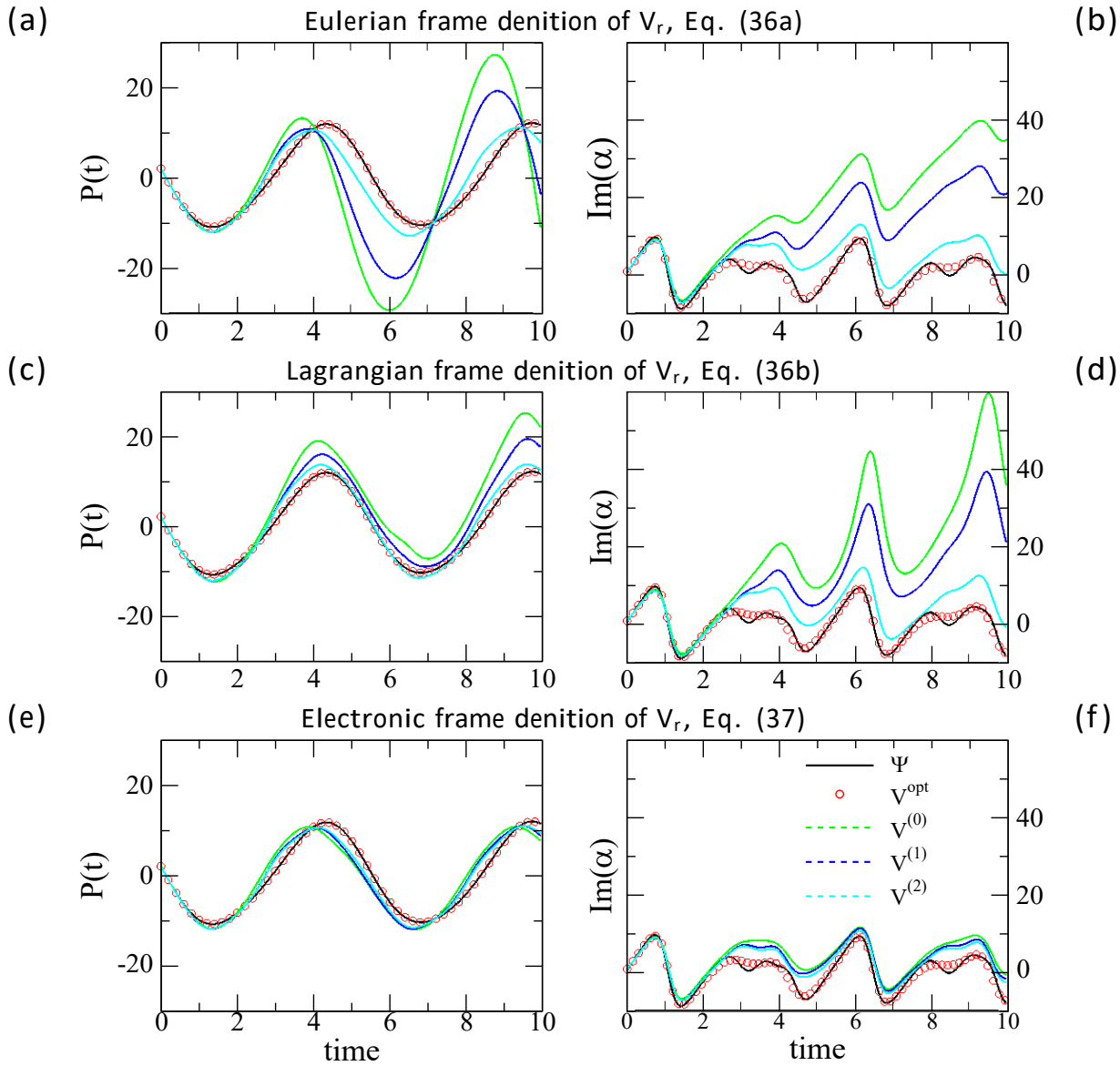

Figure 4: Dynamics with the complex norm-conserving potential dened by Eqs (36a{37). The average momenta (a,c,e) and the imaginary width parameters (b,d,f) of the nuclear wavepacket (y; t) are shown as functions of time in all panels. The results from the dynamics with all terms in V_r included ($V^{(0)}$), the electronic kinetic energy dropped ($V^{(1)}$) and all kinetic energy dropped ($V^{(2)}$) are shown as green dash, blue wide dash and cyan dot-dash, respectively. The same quantities computed for the optimal (y; t) according to Eq. (48) are indicated with red circles (V^{opt} in legend), while their counterparts p^c and =(a_{22}) of the full wavefunction (x; y; t) are shown with black solid lines (in legend) in panels (a,c,e) and (b,d,f), respectively. The same legend applies to all panels. All quantities are in the appropriate atomic units.

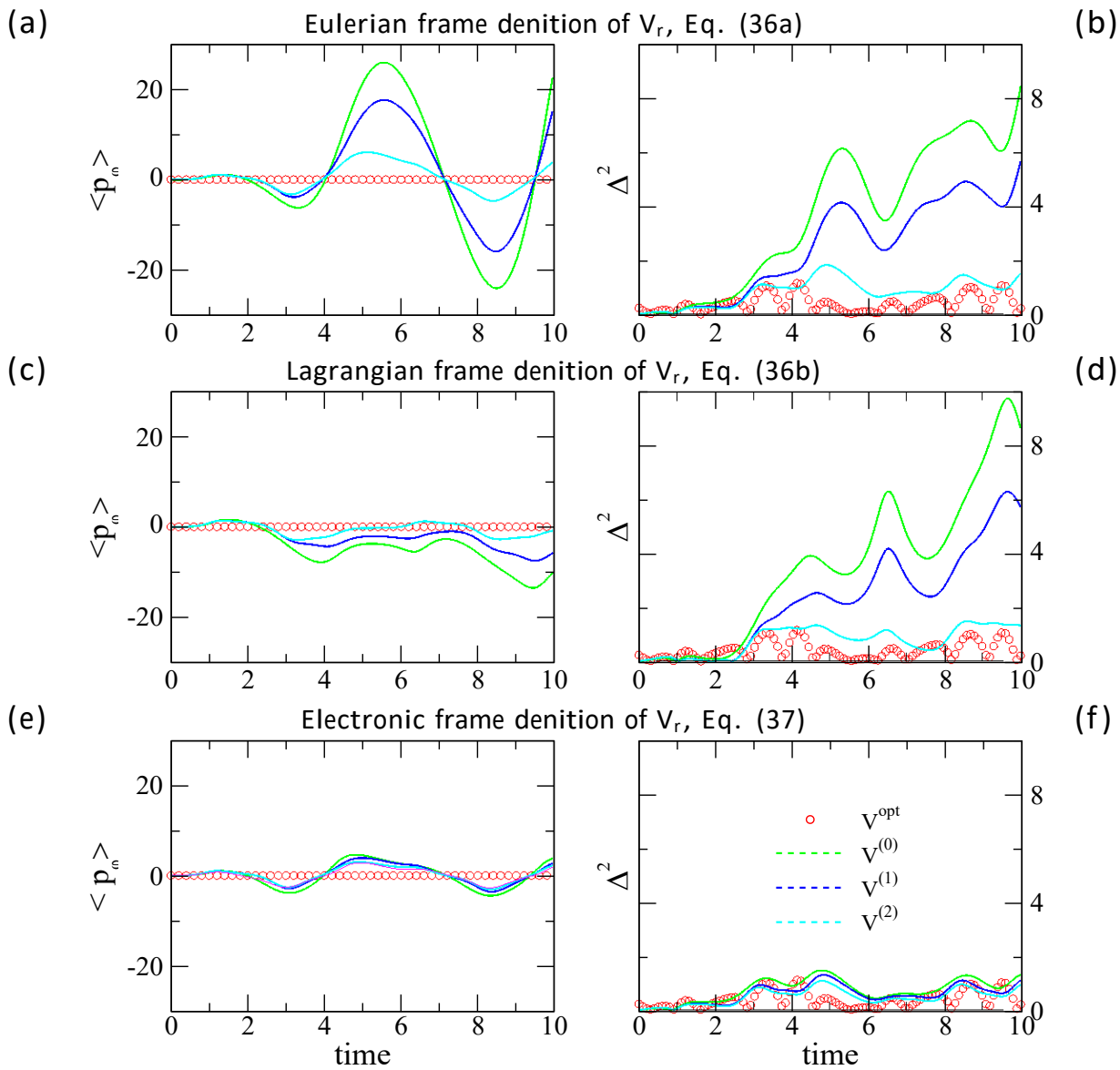

Figure 5: Dynamics with the complex norm-conserving potential dened by Eqs (36a{37). The x-averaged nuclear momentum p (in panels (a,c,e)) and its dispersion (in panels (b,d,f)) for the electronic wavepacket (y; t) are shown as functions of time in all panels. The results from the dynamics with all terms in V_r included ($V^{(0)}$), the electronic kinetic energy dropped ($V^{(1)}$) and all kinetic energy dropped ($V^{(2)}$) are shown as green dash, blue wide dash and cyan dot-dash, respectively. The same quantities computed for the optimal (y; t) according to Eq. (48) are indicated with red circles (V^{opt} in legend). The same legend applies to all panels. All quantities are given in the appropriate atomic units.

of p are closer in the former case. This means that, since the 2D wavefunction underlying the time-dependence of in all cases is the same, large deviations in p from the optimal value aord smaller deviations in dispersion, and, ideally both should be minimized in some sense. Dynamics under $V^{(2)}$ of the Lagrangian frame is better correlated with the optimal case than that of the Eulerian frame.

Lastly, let us focus on the dynamics under the intermediate or electronic-frame V_r of Eq. (37), which takes into account the y-motion of the electronic wavefunction. The results are given in Figs 4(e,f) and 5(e,f) in the same format and using the same legends as the Eulerian and Lagrangian frame cases. The main observations are: (i) neglect of the kinetic energy terms in V_r has small eect, though $V^{(2)}$ once again gives better agreement with the optimally factorized result; (ii) the discrepancy in the momentum-related quantities (Figs 4 and 5) are signicantly smaller compared to the Eulerian and Lagrangian denitions of Eqs (36a) and (36b).

3.4 Comparison to the optimal nuclear-subspace factorized dynamics

Finally, let us examine the optimal dynamics following from the stationary condition discussed in Section 2.3(c). In this case $\overline{p} = 0$, and the electronic norm is conserved with zero imaginary potential, while the real potential V_r is reconstructed from the condition on its gradient, Eq. (49), by integration. The value of the integration constant simply shifts the energy scale. Therefore, we set the constant to zero and focus on the force constant, which denes the main dynamics features, presented in Figs 6 and 7.

Overall, the action of the real (V_r) and imaginary (V_i) components of the potential V_d, decoupling the electronic and nuclear components of the full wavefunction, can be interpreted as moving the probability density by a 'ow' and by a 'source/sink' process, respectively. We assess their eect by comparing the force constants for several choices of the complex V_d. Figure 6 illustrates the time-evolution of the system of (a) the purely real V_d for the

optimal case (Eq. (48)) and (b) for one of the complex V_d, namely that of Eq. (36a) with the kinetic energy terms set to zero, referred to in Section 3.3 as $V^{(2)}$ in the Eulerian frame. In both panels the snapshots of j (y; t)j^2 are superimposed on V_r (the parabolas) for t = f0; 1; 2; 3; 4; 5g a.u.; the blue trajectory indicates the position of the wavepacket center and the red line shows the time-dependent location of the V_r minimum. Both types of dynamics come from V_r exhibiting signicant variations of the parabolic shape or, equivalently, of the force constant. These variations are interpreted as the force playing a dual role of directing the overall classical-type motion of the wavepacket center and of controlling the wavepacket spatial localization, e.g. the 'breathing' motion. Comparing the center positions (Y (t), red lines) we see sharper features in panel (a) vs (b): this dierence is compensated by the non-zero V_i in the latter case which moves the probability density by the 'source/sink' action in addition to V_r moving the probability density by 'ow'. The combined action of V_r and V_i maintains the uniform electronic normalization for any y.

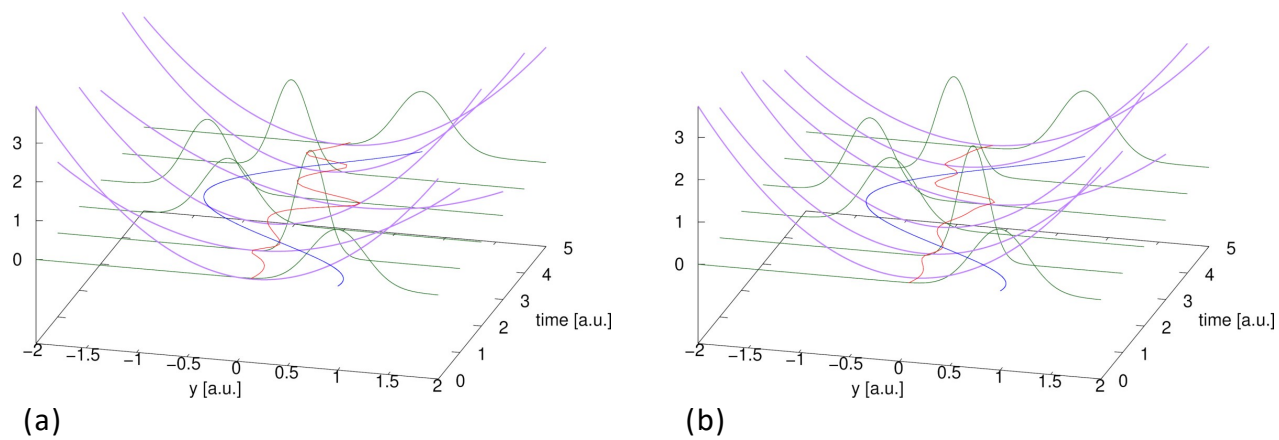

Figure 6: Dynamics with (a) the optimal real and (b) complex V_d of Eqs (48) and (36a), respectively. (The kinetic energy terms are excluded in the latter case.) In both panels the snapshots of V_r and the corresponding probability density of the nuclear wavefunction, j (y; t)j^2, are shown with purple and green lines, respectively, for t = f0; 1; 2; 3; 4; 5g a.u. The values of V_r are marked on the vertical axis. The blue lines track the position of the nuclear wavefunction center, Y (t). The minimum of V_r is indicated with the red lines.

The quadratic term of V_r, or the force constant, and of V_i are shown in Fig. 7(a,b) for all the choices of V_d examined in Section 3.3. In both panels three families of curves, generated by the dynamics with and without the kinetic energy terms under $V^{(0)}$; $V^{(1)}$ and $V^{(2)}$ as

described in Section 3.3, are shown for V_r dened in the Eulerian (Eq. (36a)), Lagrangian (Eq. (36b)) and electronic (Eq. (37)) frames of reference. The Lagrangian and the electronic frame curves are shifted up by 10 and 20 units with respect to the Eulerian frame curves. The force constant of the optimal V_r (Eq. 48) in panel (a) is shifted down by 10 units with respect to the Eulerian curves; in panel (b) the force constant of V_i, identically equal to zero in this case, is not shown. This gure clearly illustrates the deciencies of some of the V_r denitions, which as time progresses result in V_d with large coecient amplitudes. The inversion of the V_r parabolas around t = 4 a.u. (about one oscillation period) is particularly troubling. Within the limits of V_r dened as a function of y, the formulation of Eq. (37) with the kinetic energy dropped is the most stable, though neglect of the kinetic energy terms helps with stability in all situations. The purely real optimal V_d is clearly the most stable, and is attractive for conceptual and, since the dynamics with complex potentials is highly sensitive to the time-step, for practical reasons. In-depth exploration of this option, including how to extend it to multiple nuclear DOFs, will be reported in the future.

To conclude the analysis here, we have taken a closer look at the kinetic energy terms, $\langle \hat{K}_x \rangle_x = Q_x + T_x$ and $\langle \hat{D}_2 \rangle_x = Q_y + T_y$, in the denition of V_r, by isolating the contributions associated with the wavefunction amplitude and phase,

$$Q_x := \frac{\langle (r_x - \langle r_x \rangle)^2 \rangle_x}{2m}; \qquad T_x := \frac{\langle (r_x - \langle r_x \rangle)^2 \rangle_x}{2m};$$
$$Q_y := \frac{\langle (r_y - \langle r_y \rangle)^2 \rangle_x}{2M}; \qquad T_y := \frac{\langle (r_y - \langle r_y \rangle)^2 \rangle_x}{2M}. \tag{54}$$

Based on the dynamics with various combinations of the terms above, we have observed that inclusion of the quantum potential terms Q_x and/or Q_y does not change the nuclear momentum dispersion $\overline{p}$, a key characteristic of our wavefunction factorization 'quest'. As it turns out, within our model system, the analytic expression for Q_x does not depend on y, i.e. Q_x is a time-dependent constant, while the analytic formula for Q_y contains linear and quadratic in y coecients as functions of the wavepacket parameters. Interestingly, these coecients are proportional to a certain combination of the width parameters, which

within our dynamics procedure maintaining $r_y N = 0$, is equal to zero at all times. We have not tested yet if this conclusion holds for general potentials and wavefunctions, but at least it is easy to show that the forces in y-coordinate associated with Q_x and Q_y give zero contributions upon averaging over x. This suggests that, when it comes to a numerical implementation of solving both { the nuclear and the electronic TDSE (9) { for general systems, a simplied evaluation of the kinetic energy terms may be adequate.

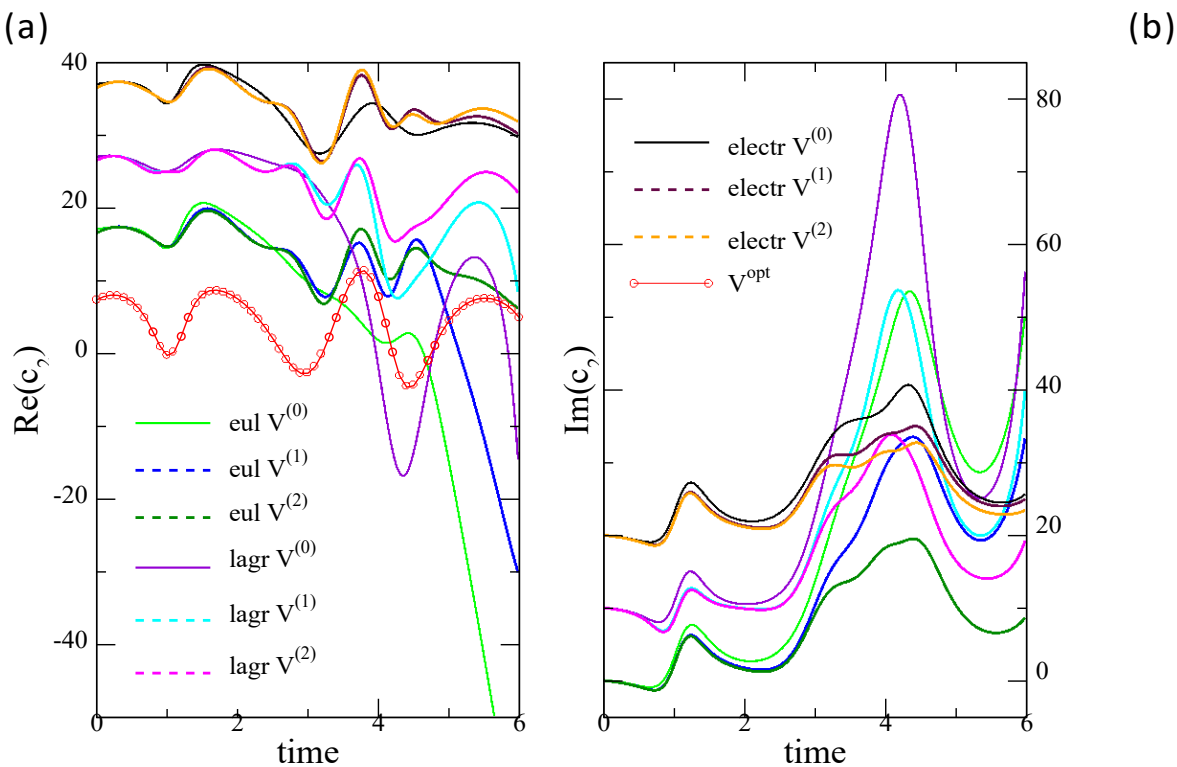

Figure 7: The quadratic coecients c_2 of V_d, represented as $V_d = \frac{c_2 y^2}{2} + c_1 y + c_0$. The real and imaginary parts of c_2, corresponding to V_r and V_i, are shown in panels (a) and (b), respectively. The legend applies to both panels. The results are obtained from V_d of Eqs (36a) (Eulerian 'eul'), (36b) (Lagrangian 'lagr', the curves shifted vertically by 10 units) and (37) (electronic frame 'electr', the curves shifted by 20 units). $<(c_2)$ following from the optimal V_r of Eq. (48) (red circles in (a)) is shifted by -10 units; $=(c_2)$ (not shown) is equal to zero by construction. The superscripts '(0)' indicate c_2 from the dynamics performed with all the terms in Eqs (36a{37) included, '(1)' { with the kinetic energy K_x, and '(2)' { with both terms, K_x and D_2, dropped from the respective V_r denitions.

4 Conclusions

Nonadiabatic dynamics (beyond a single time-independent potential energy surface) is ubiquitous in chemistry, and sometimes the nuclear quantum eects are important for understanding the chemical processes. Description of the light particles, such as electrons, as wavepackets evolving on the time-dependent potential energy surface, rather than as a superposition of a few stationary energy states, may be advantageous when numerous stationary electronic states are involved. Thus, there is a renewed interest in the wavefunction factorization methods, in large part thanks to active research in Exact Factorization with the vector potential reviewed in Ref.[41]

In this work, we have presented an exact formalism for the nuclear-subspace factorized dynamics, which connects the electronic and nuclear TDSE via a generally complex, time-dependent scalar potential V_d, that is a function of the nuclear coordinates as opposed to the methods involving the vector potential[33,34]. The dynamics potential V_d, dening the dynamics of the nuclear wavefunction component, includes the back reaction from the nuclei to electrons in a theoretically rigorous manner. Imposing the probability continuity and normalization properties on the nuclear and electronic wavefunctions, the following has been shown.

(i) The Lagrangian frame of reference, best visualized through the trajectory ow, should be dened by the gradient of the phase of the full wavefunction, averaged over the electronic DOFs.

(ii) The electronic wavefunction can be dened to have uniform normalization in the nuclear space, and the normalization will stay constant provided a specic form of the imaginary part of V_d (Eq. (34)).

(iii) There is an ambiguity in specifying the real part of V_d, which we dened to minimize the nuclear gradient of the electronic wavefunction or its energy. Several choices related to dierent frames of reference have been considered.

(iv) Finally, we have obtained a real expression for the gradient of V_d, underlying an ideal, or

optimal, factorized dynamics. In one nuclear DOF, V_d can be reconstructed as a purely real function, which is highly desirable, since the time-evolution with the imaginary potential, which 'moves' the probability dynamics via source/sink mechanism, is numerically more challenging than dynamics with real potentials.

The analysis of the various V_d options was based on the KST model of vibrationally nonadiabatic dynamics, allowing highly accurate implementation of the formalism within the Gaussian wavepacket dynamics, generalized to complex parabolic potentials. The Eulerian, Lagrangian and an intermediate 'electronic' frames of reference have been explored. It has been found that the electronic frame led to the most stable dynamics (small imaginary potential), and that the contribution from the kinetic energy terms of the electronic wavefunction was limited to the gradient of its phase. Omitting those terms altogether further stabilized the dynamics and produced the nuclear momentum of the electronic wavefunction, which was very close to the optimally factorized dynamics for a single nuclear DOF, making this choice of V_d most promising for multidimensional nuclear dynamics.

Overall, the presented nuclear subspace factorization formalism is positioned to smoothly connect to other types of trajectory-based nuclear dynamics, including the semiclassical and classical approaches, for a potentially practical time-evolution framework. Future development will include multidimensional generalizations, including search for optimal nuclear-subspace factorization procedures, and applications to more realistic electron/nuclear dynamics models.

Acknowledgement

This material is based upon work supported by the National Science Foundation under Grant CHE-1955768.

Appendix A. Conservation of the total probability density along the nuclear trajectory.

The trajectory weight denition (Eq. (20)) can be extended to the full wavefunction,

$$W_t = \int_{y_t} \quad j \quad (x; y_t; t) j^2 dx: \tag{A.1}$$

Let us dene the full wavefunction momentum components, P_x and P_y, and their normalized averages (k 2 fx; yg):

$$P_k = r^k(\arg \quad); \quad \overline{P_k} = \frac{\int P_k j \quad j^2 dx}{\int j \quad j^2 dx}: \tag{A.2}$$

The time-dependence of W_t will involve the following relations:

$$@_t j \quad j^2 = 2=(\quad (\hat{K}_x + \hat{K}_y) \quad) = \frac{r_x(P_x j \quad j^2)}{m} \quad \frac{r_y(P_y j \quad j^2)}{M}; \tag{A.3}$$

$$\frac{d}{dt} y_t = \frac{P_y \overline{y_t}}{M} = \frac{r_y P_y \overline{y_t}}{M}: \tag{A.4}$$

Using Eqs (A.2{A.4), interchanging the order of r_y with integration over x, and switching to the Lagrangian frame (the last right-hand-side term below), one obtains

$$\frac{dW_t}{dt} = \frac{y_t}{M} \int j \quad j^2 dx \; r_y(\overline{P_y}) \quad \frac{y_t}{m} \int r_x(P_x j \quad j^2) dx \; \underbrace{|}_{=0}$$
$$+ \frac{y_t}{M} \int r_y \quad P_y j \quad j^2 dx + \overline{P_y} \int r_y \quad j \quad j^2 dx \quad = 0: \tag{A.5}$$

Appendix B. Time-dependence of the average nuclear momentum of the electronic wavefunction

Starting with $@_t P_y$ of Eq. (39) and U of (40), using

$$N(y) := h \;\; j \;\; i_x$$

to label the x-averaged norm of , and denoting the expectation values over the full wave-function integrated over x as

$$\overline{P_y} := \frac{h \;\; jP_y j \;\; i_x}{N}; \quad \overline{P_y^2} := \frac{h \;\; jP_y^2 j \;\; i_x}{N}; \quad \overline{F} := \frac{h \;\; jr_y(V + U)j \;\; i_x}{N};$$

the time-dependence of $\overline{P_y}$ in the Eulerian frame is

$$\begin{aligned}
@_t\overline{P_y} &= \frac{\int (j \;\; j^2 @_t P_y + P_y @_t j \;\; j^2)dx}{N} \quad \frac{\int P_y j \;\; j^2 dx}{N} \frac{@_t N}{N} \\
&= \overline{F} \quad \frac{\int\int j \;\; j^2 r_y P_x^2 dx}{2mN} \quad \frac{\int j \;\; j^2 r_y P_y^2 dx}{2MN} \quad \frac{\int\int P_y r_x (P_x j \;\; j^2)dx}{mN} \\
&\quad \frac{\int P_y r_y (P_y j \;\; j^2)dx}{MN} \quad \frac{\int P_y j \;\; j^2 dx}{N} \quad \frac{\int r_x (P_x j \;\; j^2)dx}{mN} \quad \frac{r_y h \;\; jP_y j \;\; i_x}{MN} \\
&= \overline{F} \quad \frac{r_y h \;\; jP_y^2 j \;\; i_x}{MN} + \frac{\overline{P_y}}{M} \frac{r_y h \;\; jP_y j \;\; i_x}{N}:
\end{aligned} \tag{B.1}$$

Introducing the y-momentum standard deviation (the same whether computed for or),

$$:= \overline{P_y^2} \quad \overline{P_y}^2 \;{}^{1=2} = \overline{p^2} \quad (\overline{p})^2 \;{}^{1=2}; \tag{B.2}$$

switching to the Lagrangian frame and manipulating the gradients of the average values into the gradients of their normalized counterparts, Eq. (B.1) becomes

$$\frac{d}{dt}\overline{P_y} = \overline{F} \quad \frac{r_y \overline{P_y^2}}{M} \quad \frac{h \quad jP_y^2 j \quad i_x}{MN} \frac{r_y N}{N} + \frac{\overline{P_y}}{M} r_y \overline{P_y} + \frac{\overline{P_y}}{M} \frac{h \quad jP_y j \quad i_x}{N} \frac{r_y N}{N} + \frac{\overline{P_y}}{M} r_y \overline{P_y}$$

$$= \overline{F} \quad \frac{r_y{}^2}{M} \quad \frac{{}^2 r_y N}{M \quad N}: \tag{B.3}$$

From the nuclear TDSE the time-dependence of the nuclear momentum, p in the Lagrangian frame is given by:

$$\frac{dp}{dt} = \quad r_y (V_r + U) + \frac{\overline{p}}{M} r_y p \quad ; \tag{B.4}$$

where

$$U = \frac{r_y^2 j \quad j}{2Mj \quad j}; \tag{B.5}$$

is the appropriate quantum potential. Then, the time-evolution of the average electronic momentum in the nuclear DOF, $\overline{p} = \overline{P_y} \quad p$, is governed by,

$$\frac{d\overline{p}}{dt} = F_d \quad \frac{\overline{p}}{M} r_y p \quad ; \tag{B.6}$$

where F_d includes the dispersion-related forces,

$$F_d := \frac{hjr_y(V+U)ji_x}{N(y)} \quad r_y{}^2 \frac{{}^2}{M} \quad \frac{}{M} \frac{r_y j \quad j^2}{j \quad j^2} + r_y (V_r + U): \tag{B.7}$$

Its Eulerian frame counterpart, based on Eq. (39) and the equation of motion for p , is given for completeness,

$$@_t p = \quad r_y (V + U) \quad \frac{p}{M} r p \quad ; \tag{B.8}$$

$$\overline{@_t p} = F_d \frac{r_y \overline{(p)^2}}{2M} \quad \frac{r_y (p \overline{p})}{M}: \tag{B.9}$$

To obtain Eq. (B.6), the average of $r_y U$, which denes the quantum force associated with the full wavefunction (x; y; t) = (x; y; t) (y; t), was evaluated and simplied as follows.

Let us separate U into four contributions:

$$U = U_x + U_c + U + U \; ; \tag{B.10}$$

$$U_x = \frac{r_x^2 \, jj}{2m\,jj} ; \tag{B.11}$$

$$U_c = \frac{r}{M} \frac{r_y \, jj}{jj} ; \tag{B.12}$$

$$U = \frac{r_y^2 \, jj}{2M\,jj} ; \tag{B.13}$$

$$U = \frac{r_y^2 j \;\; j}{2M\, j \;\; j} : \tag{B.14}$$

Using

$$N(y) = \int jj^2 dx; \quad r = \frac{r_y j \;\; j}{j}; \quad r = jj \frac{r_y jj \; j}{}; \quad$$

the rst three terms simplify as:

$$\int jj^2 r_y U_x dx = \frac{1}{} \int jj \; {}^2 \frac{r_y r_{xx} jj}{jj} \frac{r_{xx}^2 jj r_y jj \;\; 2M}{jj^2} dx$$

$$[\text{integrate by parts}] = \frac{1}{2M} \left(r_x jj r_{yx} j^2 j + r_{xy} jj r_x^2 jj \right) dx = 0; \tag{B.15}$$

$$\int jj^2 r_y U_c dx = \frac{1}{M} \int jj^2 r_y \, r \frac{r_y jj}{jj} dx$$

$$= \frac{r_y r}{M} \int jj^2 \frac{r_y jj}{jj} dx \quad \frac{r_y jj}{M} \int jj^2 r_y \frac{j}{jj} \frac{r_y j}{} dx \tag{B.16} = \frac{}{2M}$$

$$r_y N(y) \, r \quad \frac{r_y r}{M} \underbrace{\{z}_{\text{use } r_y N(y)=0} \quad \frac{r}{} \int jj r^2 jj \; (r_y jj)^2 dx = \frac{}{M} \underbrace{\{z}_{\text{use } r_y N(y)=0} \; hjr^2 ji_x ;$$

$$\int jj^2 r_y U dx = \frac{1}{2M} \int jj^2 r_y \frac{j}{jj_y^2 j} dx$$

$$= \frac{1}{2M} \underbrace{\{z}_{\text{use } r_y^3 N(y)=0} \; jjr_y jj^3 \quad r_y^3 jjr_y jj dx = \frac{r_y hjrji_x \;\; {}^2}{M} \tag{B.17}$$

With that Eq. (B.6) is equivalent to

$$\frac{d\overline{p}}{dt} = r_y V_r \quad \frac{hjr_y V ji_x}{N(y)} \quad \frac{(2r + r_y)hjrji_x^2}{MN(y)} \quad \frac{(2r + r_y)^2}{M} \quad p\frac{\overline{r_y p}}{M} : \tag{B.18}$$

Appendix C. Time-evolution of a Gaussian wavefunction in an N_d-dimensional complex quadratic potential

Take an N_d-dimensional Gaussian wavepacket in atomic units (~ = 1),

$$(x; t) = N_0 \exp(\quad (x \quad x_t^c) A_t (x \quad x_t^c)=2 + \{p_t^c (x \quad x_t^c) + \{s_t + {}_t) : \tag{C.1}$$

where the subscript t indicates functions dependent only on time t. N_0 is the initial normalization constant and chosen such that at t = 0 we have $_0$ = 0, and is given as

$$N_0 = \frac{\det <(A_0)^{1=4}}{N_d} : \tag{C.2}$$

The parameters x_t^c and p_t^c are real N_d-dimensional vectors, describing the wavepacket center and s_t describes the coordinate-independent phase. The nal parameter A_t is a complex matrix with real and imaginary parts:

$$A = A_< + \{A_= : \tag{C.3}$$

The wavefunction evolves according to the Hamiltonian,

$$\hat{H} = \frac{1}{2} \hat{p}^T M \quad {}^1 \hat{p} + V(x); \tag{C.4}$$

M is a diagonal matrix of particle masses. $V(x)$ is the complex, possibly, time-dependent quadratic potential with real and imaginary parts, $V_r(x)$ and $V_i(x)$,

$$V(x) = V_r(x) + \{V_i(x): \tag{C.5}$$

The TDSE yields the following equations of motion for the wavepacket parameters,

$$\{\frac{dA}{dt} = AM^{-1}A - \nabla\nabla^T V; \tag{C.6a}$$

$$\frac{dx^c}{dt} = M^{-1}p_c + A_< {}^{-1}\nabla V_i(x^c); \tag{C.6b}$$

$$\frac{dp^c}{dt} = -\nabla V_r(x^c) - A_= A_<{}^{-1}\nabla V_i(x^c); \tag{C.6c}$$

$$\frac{d}{dt} = \frac{1}{2}\mathrm{Tr}\,A_= M^{-1} + V_i(x^c) \tag{C.6d}$$

$$\frac{ds}{dt} = \frac{1}{2}(p^c)^T M^{-1} p^c - V_r(x^c) - \frac{1}{2}\mathrm{Tr}\,A_< M^{-1} + (p^c)^T A_<{}^{-1}\nabla V_i(x^c): \tag{C.6e}$$

where $\nabla\nabla^T V$ is the (coordinate-independent) Hessian matrix of the potential V.

The total wavefunction energy is,

$$E = \langle \psi | H | \psi \rangle = \frac{1}{2}(p^c)^T M^{-1} p^c + V(x^c) + \frac{1}{4}\mathrm{Tr}\,A_<{}^{-1}\nabla\nabla^T V + K + U; \tag{C.7}$$

where the first two right-hand-side terms are the classical kinetic and potential energy of the wavefunction center, the third right-hand-side term is the potential energy contribution from wavefunction delocalization. The last two right-hand-side terms K and U are given below and describe the kinetic energy from the derivatives of the wavefunction phase and amplitude respectively,

$$K := \frac{1}{4}\mathrm{Tr}(A_= A_<{}^{-1} A_= M^{-1}); \quad U := \frac{1}{4}\mathrm{Tr}(A^< M^{-1}): \tag{C.8}$$

References

(1) Lau, J. A.; Choudhury, A.; Li, C.; Schwarzer, D.; Verma, V. B.; Wodtke, A. M. Observation of an Isomerizing Double-Well Quantum System in the Condensed Phase. Science 2020, 367, 175{178.

(2) Borodin, D.; Hertl, N.; Park, G. B.; Schwarzer, M.; Fingerhut, J.; Wang, Y.; Zuo, J.; Nitz, F.; Skoulatakis, G.; Kandratsenka, A.; Auerbach, D. J.; Schwarzer, D.; Guo, H.; Kitsopoulos, T. N.; Wodtke, A. M. Quantum Eects in Thermal Reaction Rates at Metal Surfaces. Science 2022, 377, 394{398.

(3) Dutra, M.; Amaya, J. A.; McElhenney, S.; Manley, O. M.; Makris, T. M.; Rassolov, V.; Garashchuk, S. Experimental and Theoretical Examination of the Kinetic Isotope Eect in Cytochrome P450 Decarboxylase OleT. J. Phys. Chem. B 2022, 126, 3493{3504.

(4) Rodriguez, J. D.; Gonzalez, M. G.; Rubio-Lago, L.; Banares, L. Direct Evidence of Hydrogen Transfer (ESHT) Reaction of Phenol- Ammonia Clusters. Phys. Chem. Chem. Phys. 2014, 16, 3757{3762.

(5) Gatti, F., Ed. Molecular Quantum Dynamics: From Theory to Applications; Springer, 2014.

(6) Meyer, H. D.; Manthe, U.; Cederbaum, L. S. the Multi-Congurational Time-Dependent Hartree Approach. Chem. Phys. Lett. 1990, 165, 73 { 78.

(7) Burghardt, I.; Meyer, H.-D.; Cederbaum, L. S. Approaches to the Approximate Treatment of Complex Molecular Systems by the Multiconguration Time-Dependent Hartree Method. J. Chem. Phys. 1999, 111, 2927{2939.

(8) Meyer, H. D.; Worth, G. A. Quantum Molecular Dynamics: Propagating Wavepackets and Density Operators Using the Multiconguration Time-Dependent Hartree Method. Theor. Chem. Acc. 2003, 109, 251{267.

(9) Light, J. C.; Carrington Jr., T. Advances in Chemical Physics; John Wiley & Sons, Ltd, 2000; pp 263{310.

(10) Wang, H. B.; Thoss, M. Multilayer Formulation of the Multiconguration Time-Dependent Hartree Theory. J. Chem. Phys. 2003, 119, 1289{1299.

(11) Vendrell, O.; Gatti, F.; Meyer, H.-D. Full Dimensional (15 Dimensional) Quantum-Dynamical Simulation of the Protonated Water-Dimer IV: Isotope Eects in the Infrared Spectra of D(D2O)2+, H(D2O)2+, and D(H2O)2+ Isotopologues. J. Chem. Phys. 2009, 131, 034308.

(12) Schroeder, M.; Gatti, F.; Meyer, H.-D. Theoretical Studies of the Tunneling Splitting of Malonaldehyde Using the Multiconguration Time-Dependent Hartree Approach. J. Chem. Phys. 2011, 134.

(13) Hammer, T.; Manthe, U. Iterative Diagonalization in the State-Averaged Multi-Congurational Time-Dependent Hartree Approach: Excited State Tunneling Splittings in Malonaldehyde. J. Chem. Phys. 2012, 136, 054105.

(14) Richings, G.; Polyak, I.; Spinlove, K.; Worth, G.; Burghardt, I.; Lasorne, B. Quantum Dynamics Simulations Using Gaussian Wavepackets: the VMCG Method. Int. Rev. Phys. Chem. 2015, 34, 269{308.

(15) Coonjobeeharry, J.; Spinlove, K. E.; Sanz Sanz, C.; Sapunar, M.; Doslic, N.; Worth, G. A. Mixed-Quantum-Classical or Fully-Quantized Dynamics? A Unied Code to Compare Methods. Philos. Trans. Royal Soc. A 2022, 380, 20200386.

(16) Miller, W. H. the Semiclassical Initial Value Representation: A Potentially Practical Way for Adding Quantum Eects to Classical Molecular Dynamics Simulations. J. Phys. Chem. A 2001, 105, 2942{2955.

(17) Liu, J.; Miller, W. H. Linearized Semiclassical Initial Value Time Correlation Functions Using the Thermal Gaussian Approximation: Applications to Condensed Phase Systems. J. Chem. Phys. 2007, 127, 114506.

(18) Habershon, S.; Manolopoulos, D. E.; Markland, T. E.; Miller, T. F. Ring-Polymer Molecular Dynamics: Quantum Eects in Chemical Dynamics from Classical Trajectories in an Extended Phase Space. Ann. Rev. Phys. Chem. 2013, 64, 387{413.

(19) Ananth, N. Mapping Variable Ring Polymer Molecular Dynamics: A Path-Integral Based Method for Nonadiabatic Processes. J. Chem. Phys. 2013, 139, 124102.

(20) Richardson, J. O.; Thoss, M. Communication: Nonadiabatic Ring-Polymer Molecular Dynamics. J. Chem. Phys. 2013, 139, 031102.

(21) Garashchuk, S.; Rassolov, V.; Prezhdo, O. Reviews in Computational Chemistry; Wiley, 2011; Vol. 27; Chapter Semiclassical Bohmian Dynamics, pp 111{210.

(22) Althorpe, S. C. Path-Integral Approximations to Quantum Dynamics. Eur. Phys. J. B 2021, 94, 155.

(23) Shalashilin, D. V.; Child, M. S. Real Time Quantum Propagation on a Monte Carlo Trajectory Guided Grids of Coupled Coherent States: 26D Simulation of Pyrazine Absorption Spectrum. J. Chem. Phys. 2004, 121, 3563{3568.

(24) Makhov, D. V.; Glover, W. J.; Martinez, T. J.; Shalashilin, D. V. Ab Initio Multiple Cloning Algorithm for Quantum Nonadiabatic Molecular Dynamics. J. Chem. Phys. 2014, 141, 054110.

(25) Saller, M. A. C.; Habershon, S. Quantum Dynamics with Short-Time Trajectories and Minimal Adaptive Basis Sets. J. Chem. Theory Comput. 2017, 13, 3085{3096.

(26) Wyatt, R. E. Quantum Dynamics with Trajectories: Introduction to Quantum Hydrodynamics; Springer-Verlag, 2005.

(27) Schi, J.; Poirier, B. Communication: Quantum Mechanics Without Wavefunctions. J. Chem. Phys. 2012, 136, 031102.

(28) Acosta-Matos, Juan Carlos and Meier, Christoph and Martnez-Mesa, Aliezer and Uranga-Piña, Llinersy, Eective Phase Space Representation of the Quantum Dynamics of Vibrational Predissociation of the ArBr2(B,v =16•••25) Complex. J. Phys. Chem. A 2022, 126, 1805{1815.

(29) Agostini, F.; Curchod, B. F. E. Chemistry Without the Born-Oppenheimer Approximation. Philos. Trans. Royal Soc. A 2022, 380, 20200375.

(30) Vindel-Zandbergen, P.; Matsika, S.; Maitra, N. T. Exact-Factorization-Based Surface Hopping for Multistate Dynamics. J. Phys. Chem. Lett. 2022, 13, 1785{1790.

(31) Talotta, F.; Morisset, S.; Rougeau, N.; Lauvergnat, D.; Agostini, F. Internal Conversion and Intersystem Crossing with the Exact Factorization. J. Chem. Theory Comput. 2020, 16, 4833{4848.

(32) Cederbaum, L. S. Erratum: \the Exact Molecular Wavefunction As a Product of an Electronic and a Nuclear Wavefunction" [J. Chem. Phys. 138, 224110 (2013)]. J. Chem. Phys. 2014, 141, 029902.

(33) Abedi, A.; Maitra, N. T.; Gross, E. K. U. Correlated Electron-Nuclear Dynamics: Exact Factorization of the Molecular Wavefunction. J. Chem. Phys. 2012, 137, 22A530.

(34) Abedi, A.; Maitra, N. T.; Gross, E. Exact Factorization of the Time-Dependent Electron-Nuclear Wave Function. Phys. Rev. Lett. 2010, 105, 123002.

(35) Agostini, F.; Abedi, A.; Suzuki, Y.; Gross, E. Mixed Quantum-Classical Dynamics on the Exact Time-Dependent Potential Energy Surface: A Fresh Look at Non-Adiabatic Processes. Mol. Phys. 2013, 111, 3625{3640.

(36) Abedi, A.; Agostini, F.; Suzuki, Y.; Gross, E. K. U. Dynamical Steps That Bridge Piecewise Adiabatic Shapes in the Exact Time-Dependent Potential Energy Surface. Phys. Rev. Lett. 2013, 110, 263001.

(37) Min, S. K.; Agostini, F.; Gross, E. K. U. Coupled-Trajectory Quantum-Classical Approach to Electronic Decoherence in Nonadiabatic Processes. Phys. Rev. Lett. 2015, 115, 073001.

(38) Kohen, D.; Stillinger, F. H.; Tully, J. C. Model Studies of Nonadiabatic Dynamics. J. Chem. Phys. 1998, 109, 4713{4725.

(39) Bohm, D. A Suggested Interpretation of the Quantum Theory in Terms of "hidden" Variables, I and II. Phys. Rev. 1952, 85, 166{193.

(40) Garashchuk, S.; Rassolov, V. A. Semiclassical Dynamics with Quantum Trajectories: Formulation and Comparison with the Semiclassical Initial Value Representation Propagator . J. Chem. Phys. 2003, 118, 2482{2490.

(41) Villaseco Arribas, E.; Agostini, F.; Maitra, N. T. Exact Factorization Adventures: A Promising Approach for Non-Bound States. Molecules 2022, 27.

(42) Tannor, D. J. Introduction to Quantum Mechanics: A Time-Dependent Perspective; University Science Books, 2006.

Graphical TOC Entry